

Achievable Rate Optimization for Large Stacked Intelligent Metasurfaces Based on Statistical CSI

Anastasios Papazafeiropoulos, Pandelis Kourtessis, Symeon Chatzinotas, Dimitra I. Kaklamani, Iakovos S. Venieris

Abstract—Stacked intelligent metasurface (SIM) is an emerging design that consists of multiple layers of metasurfaces. A SIM enables holographic multiple-input multiple-output (HMIMO) precoding in the wave domain, which results in the reduction of energy consumption and hardware cost. On the ground of multiuser beamforming, this letter focuses on the downlink achievable rate and its maximization. Contrary to previous works on multiuser SIM, we consider statistical channel state information (CSI) as opposed to instantaneous CSI to overcome challenges such as large overhead. Also, we examine the performance of large surfaces. We apply an alternating optimization (AO) algorithm regarding the phases of the SIM and the allocated transmit power. Simulations illustrate the performance of the considered large SIM-assisted design as well as the comparison between different CSI considerations.

Index Terms—Reconfigurable intelligent surface (RIS), stacked intelligent metasurfaces (SIM), 6G networks.

I. INTRODUCTION

The technology of reconfigurable intelligent surfaces (RISs) has recently emerged to increase coverage and enhance spectral and energy efficiencies in various communication environments [1], [2]. In general terms, an RIS includes a surface that includes a large number of elements, which are nearly passive and have low cost. The purpose of these elements is to adjust the phases of the incident electromagnetic (EM) waves by using a smart controller, and hence, shape the propagation environment dynamically [3]–[5].

However, most existing works on RIS assume single-layer metasurface structure [3], [4], [6], which imposes a constraint on the adjustment of the beam patterns. Also, the single-layer structures of RISs do not have the capability of inter-user interference suppression as shown in [6]. These observations led the authors in [7], [8] to propose a stacked intelligent metasurface (SIM), which consists of an array of programmable metasurfaces similar to artificial neural networks (ANNs). Among the processing capabilities of a SIM, we that the forward propagation takes place at the speed of light.

On this ground, in [7], authors proposed a SIM-based design for the transceiver of point-to-point multiple-input multiple-output (MIMO) communication systems, where the combining and the precoding take place as the EM waves propagate along the SIM. In [8], we observe the integration of a SIM to the transmitter, i.e., the base station (BS) towards enabling beamforming in the EM domain based on instantaneous channel state information (CSI). Contrary to [7] and [8], in [9] and [10], we proposed more general hybrid digital wave designs, where

A. Papazafeiropoulos is with the Communications and Intelligent Systems Research Group, University of Hertfordshire, Hatfield AL10 9AB, U. K., and with SnT at the University of Luxembourg, Luxembourg. P. Kourtessis is with the Communications and Intelligent Systems Research Group, University of Hertfordshire, Hatfield AL10 9AB, U. K. S. Chatzinotas is with the SnT at the University of Luxembourg, Luxembourg. Dimitra I. Kaklamani is with the Microwave and Fiber Optics Laboratory, and Iakovos S. Venieris is with the Intelligent Communications and Broadband Networks Laboratory, School of Electrical and Computer Engineering, National Technical University of Athens, Zografou, 15780 Athens, Greece. Corresponding author's email: tapapazaf@gmail.com.

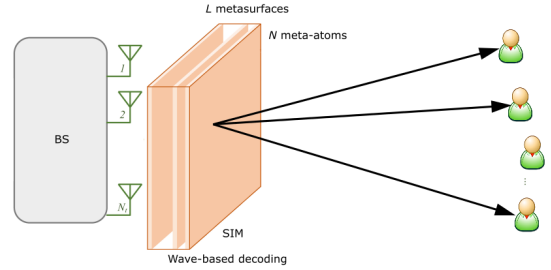


Fig. 1: A SIM-aided MIMO system.

all element parameters are optimised simultaneously through more efficient algorithms.

In this work, we focus on a SIM-enabled multiuser architecture operating solely in the wave domain. Note that [10] assumes a hybrid digital wave design, and [11] focuses on satellite communication systems. Also, contrary to previous works [7]–[9], we consider a SIM that consists of large metasurfaces, since we apply the use-and-then-forget (UatF) bound [12]. Most importantly, we obtain the downlink rate and perform its optimization regarding the phase shifts and transmit power in terms of statistical CSI. Notably, this approach enables the optimization at every several coherence intervals rather than optimizing at each interval. Hence, we achieve lower overhead, which is one of the main challenges in SIM-assisted systems.

Notation: Matrices and vectors are represented by boldface upper and lower case symbols, respectively. The notations $(\cdot)^T$, $(\cdot)^H$, and $\text{tr}(\cdot)$ denote the transpose, Hermitian transpose, and trace operators, respectively. Also, the symbol $\mathbb{E}[\cdot]$ denotes the expectation operator. The floor function $\lfloor x \rfloor$ gives as output the greatest integer less than or equal to x . The notation $\text{diag}(\mathbf{A})$ represents a vector with elements equal to the diagonal elements of \mathbf{A} . The notation $\mathbf{b} \sim \mathcal{CN}(\mathbf{0}, \mathbf{\Sigma})$ represents a circularly symmetric complex Gaussian vector with zero mean and a covariance matrix $\mathbf{\Sigma}$.

II. SYSTEM MODEL

We consider a SIM-aided MIMO communication system as depicted in Fig. 1. In particular, a BS, which includes N_t antennas, communicates with K single-antenna user equipments (UEs) through a SIM performing wave-based processing. The SIM is implemented by L metasurfaces, where each one has a large number of N meta-atoms. Let $\mathcal{K} = \{1, \dots, K\}$, $\mathcal{L} = \{1, \dots, L\}$, and $\mathcal{N} = \{1, \dots, N\}$ denote the sets of UEs, metasurfaces, and meta-atoms, respectively. Note that an intelligent controller adjusts the shifts of the phases of the electromagnetic (EM) waves that impinge on the metasurface layers.

On this basis, let $\theta_n^l \in [0, 2\pi)$, $n \in \mathcal{N}$, $l \in \mathcal{L}$ be the phase shift by the n th meta-atom on the surface layer l . Also, we denote $\phi_n^l = e^{j\theta_n^l}$, and $\mathbf{\Phi}_l = \text{diag}(\phi^l) \in \mathbb{C}^{N \times N}$, where $\phi^l =$

$[\phi_1^l, \dots, \phi_N^l]^\top \in \mathbb{C}^{N \times 1}$.¹ In addition, $\mathbf{W}^l \in \mathbb{C}^{N \times N}$, $l \in \mathcal{L}/\{1\}$ denotes the coefficient matrix between layer $(l-1)$ and layer l . In particular, its entries from meta-atom \tilde{n} on layer $(l-1)$ to meta-atom n on layer l , $\forall l \in \mathcal{L}$ are given by

$$w_{n,\tilde{n}}^l = \frac{A_t \cos x_{n,\tilde{n}}^l}{r_{n,\tilde{n}}^l} \left(\frac{1}{2\pi r_{n,\tilde{n}}^l} - j \frac{1}{\lambda} \right) e^{j2\pi r_{n,\tilde{n}}^l / \lambda}, \quad (1)$$

where A_t is the area of each meta-atom at the SIM, $x_{n,\tilde{n}}^l$ denotes the angle between the normal direction of the transmit metasurface layer $(l-1)$ and the propagation direction, $r_{n,\tilde{n}}^l$ is the respective transmission distance. Moreover, let $\mathbf{w}_k^1 \in \mathbb{C}^{N \times 1}$ express the coefficient from the transmit antenna array. Thus, the impact of the SIM can be expressed as

$$\mathbf{G} = \Phi_L \mathbf{W}^L \dots \Phi_2 \mathbf{W}^2 \Phi_1 \in \mathbb{C}^{N \times N}. \quad (2)$$

Let $\mathbf{h}_k \in \mathbb{C}^{N \times 1}$, $\forall k \in \mathcal{K}$ express the channel between the last layer and UE k that is described by the correlated Rician fading distribution as

$$\mathbf{h}_k = \sqrt{\beta_k} \left(\sqrt{\frac{\kappa_k}{1+\kappa_k}} \mathbf{h}_{k,\text{LoS}} + \sqrt{\frac{1}{1+\kappa_k}} \mathbf{h}_{k,\text{NLoS}} \right) \quad \forall k \in \mathcal{K}. \quad (3)$$

In (3), κ_k is the Rician factor, β_k is the channel gain, $\mathbf{h}_{k,\text{NLoS}} \in \mathbb{C}^{N \times 1}$ is the LoS component, and $\mathbf{h}_{k,\text{NLoS}} \sim \mathcal{CN}(\mathbf{0}, \mathbf{R}) \in \mathbb{C}^{N \times N}$ is the NLoS component with $\mathbf{R} \in \mathbb{C}^{N \times N}$ representing the spatial correlation of each surface. This correlation is obtained $\forall n \in \mathcal{N}$, $\tilde{n} \in \mathcal{N}$ as [14]

$$[\mathbf{R}_{\text{SIM}}]_{\tilde{n},n} = \text{sinc}(2\|\mathbf{u}_n - \mathbf{u}_{\tilde{n}}\|/\lambda), n, \tilde{n} = 1, \dots, N \quad (4)$$

where $\mathbf{u}_n = [0, i(n)d_H, j(n)d_V]^\top$ with $i(n) = \text{mod}(n-1, N_x)$ and $j(n) = \lfloor (n-1)/N_x \rfloor$ being the horizontal and vertical indices of element n , respectively. N_x and N_y are the elements per row and column, while d_H and d_V denote the horizontal width and the vertical height.

III. DOWNLINK DATA TRANSMISSION

During the downlink transmission and based on wave-based beamforming [8], the received signal at the k -th UE is written as

$$y_k = \mathbf{h}_k^H \mathbf{G} \sum_{i=1}^K \mathbf{w}_i^1 \sqrt{p_i} x_i + n_k, \quad \forall k \in \mathcal{K} \quad (5)$$

where x_i is the information symbol intended for the k -th UE, which has a zero mean and unit variance. Also, p_i is the power corresponding to the k -th UE with $\sum_{i=1}^K p_i \leq P_T$, where P_T is the total transmit power at the BS. Also $n_k \sim \mathcal{CN}(0, \sigma_k^2)$ denotes the additive white Gaussian noise (AWGN) with σ_k^2 expressing its variance at UE k .

The downlink achievable SE of UE k is given by

$$\text{SE} = \sum_{k=1}^K \log_2(1 + \gamma_k), \quad (6)$$

¹Herein, we consider phase shifts, which are continuously-adjustable and their modulus equals to 1 to evaluate large SIM-aided MIMO communications. Practical issues such as the consideration of discrete phase shifts [13] is the topic of future work.

where γ_k denotes the downlink signal-to-interference-plus-noise ratio (SINR), which is written according to the UaTF bounding technique [12] as

$$\gamma_k = \frac{p_k |\mathbb{E}\{\mathbf{h}_k^H \mathbf{G} \mathbf{w}_k^1\}|^2}{\sum_{i=1}^K p_i \mathbb{E}\{|\mathbf{h}_k^H \mathbf{G} \mathbf{w}_i^1|^2\} - p_k |\mathbb{E}\{\mathbf{h}_k^H \mathbf{G} \mathbf{w}_k^1\}|^2 + \sigma_k^2}, \quad (7)$$

where is assumed that UE k has knowledge of the average effective channel.

Proposition 1: The achievable SINR of UE k for a given SIM during the downlink transmission is provided by (8).

Proof: The numerator becomes

$$|\mathbb{E}\{\mathbf{h}_k^H \mathbf{G} \mathbf{w}_k^1\}|^2 = \beta_k \frac{\kappa_k}{1+\kappa_k} |\mathbf{h}_{k,\text{LoS}}^H \mathbf{G} \mathbf{w}_k^1|^2. \quad (9)$$

Regarding the denominator of (7), the first term is written as

$$\mathbb{E}\{|\mathbf{h}_k^H \mathbf{G} \mathbf{w}_i^1|^2\} = \text{tr}(\mathbf{h}_k^H \mathbf{G} \mathbf{w}_i^1 \mathbf{w}_i^{1H} \mathbf{G}^H \mathbf{h}_k) \quad (10)$$

$$= \beta_k \frac{1}{1+\kappa_k} \text{tr}(\mathbf{G} \mathbf{w}_i^1 \mathbf{w}_i^{1H} \mathbf{G}^H \mathbf{R}) \\ + \beta_k \frac{\kappa_k}{1+\kappa_k} \mathbf{h}_{k,\text{LoS}}^H \mathbf{G} \mathbf{w}_i^1 \mathbf{w}_i^{1H} \mathbf{G}^H \mathbf{h}_{k,\text{LoS}}, \quad (11)$$

where, in (10), we have applied that $\mathbf{x}^H \mathbf{y} = \text{tr}(\mathbf{y} \mathbf{x}^H)$ for any vectors \mathbf{x} , \mathbf{y} . By substituting (9) and (11) in (7), we obtain the achievable SINR. ■

IV. PROBLEM FORMULATION AND OPTIMIZATION

The maximization of the sum SE regarding the phase shifts of each surface and the allocated power is of great importance.

A. Problem Formulation

The maximization problem is formulated as

$$(\mathcal{P}) \quad \max_{\phi_l, \mathbf{p}} f(\phi_l, \mathbf{p}) = \sum_{k=1}^K \log_2 \left(1 + \frac{D_k}{I_k} \right) \quad (12a)$$

$$\text{s.t.} \quad \mathbf{G} = \Phi_L \mathbf{W}^L \dots \Phi_2 \mathbf{W}^2 \Phi_1, \quad (12b)$$

$$\Phi_l = \text{diag}(\phi_1^l, \dots, \phi_N^l), l \in \mathcal{L}, \quad (12c)$$

$$|\phi_n^l| = 1, n \in \mathcal{N}, l \in \mathcal{L}, \quad (12d)$$

$$\sum_{i=1}^K p_i = P_T \quad (12e)$$

$$p_k \geq 0, \forall k \in \mathcal{K}, \quad (12f)$$

where D_k and I_k are the numerator and denominator of γ_k obtained in Proposition 1. Also, we have defined the vector $\mathbf{p} = [p_1, \dots, p_K]^\top$. Note that the constraint (12d) expresses that each RIS element provides only a phase shift while (12e) corresponds to the maximum power constraint.

The non-convexity optimization problem (\mathcal{P}) and its dependence on the unit-modulus constraint with respect to ϕ_l make the solution challenging. For this reason, we resort to alternating optimization (AO). According to this technique, ϕ_l and \mathbf{p} will be optimized individually in an iterative manner. Specifically, first, we find the optimum ϕ_l for a fixed \mathbf{p} . During the next step, we solve for \mathbf{p} with ϕ_l fixed. The objective converges to its optimum value by iterating this process, which leads to the increase of $f(\phi_l, \mathbf{p})$ after each step until a specific point because of the upper-bound coming from the power constraint (12e).

$$\gamma_k = \frac{p_k \kappa_k |\mathbf{h}_{k,\text{LoS}}^H \mathbf{G} \mathbf{w}_k^1|^2}{\sum_{i=1}^K p_i \text{tr}(\mathbf{G} \mathbf{w}_i^1 \mathbf{w}_i^{1H} \mathbf{G}^H \mathbf{R}) + \sum_{i \neq k}^K p_i \kappa_k \mathbf{h}_{k,\text{LoS}}^H \mathbf{G} \mathbf{w}_i^1 \mathbf{w}_i^{1H} \mathbf{G}^H \mathbf{h}_{k,\text{LoS}} + \frac{\sigma_k^2(1+\kappa_k)}{\beta_k}}. \quad (8)$$

B. SIM Optimization

Until now, ϕ_l was assumed fixed. However, to exploit each metasurface towards wave-based beamforming while maximizing (6), the optimization of each ϕ_l has to take place. Its presence is observed inside the matrix \mathbf{G} , appearing in D_k and I_k . Hence, the maximization problem regarding ϕ_l is described as

$$(\mathcal{P}1) \quad \max_{\phi_l} f(\phi_l) \quad (13a)$$

$$\text{s.t.} \quad \mathbf{G} = \Phi_L \mathbf{W}^L \dots \Phi_2 \mathbf{W}^2 \Phi_1, \quad (13b)$$

$$\Phi_l = \text{diag}(\phi_1^l, \dots, \phi_N^l), l \in \mathcal{L}, \quad (13c)$$

$$|\phi_n^l| = 1, n \in \mathcal{N}, l \in \mathcal{L}, \quad (13d)$$

where the maximization problem ($\mathcal{P}1$) is non-convex regarding ϕ_l , and it obeys to a unit-modulus constraint with respect to ϕ_n^l . Application of the projected gradient ascent algorithm until convergence while taking into account the unit-modulus constraint results in a locally optimal solution to ($\mathcal{P}1$).

The proposed algorithm suggests starting from ϕ_l^0 , and then shifting along the gradient of $f(\phi_l)$. The new point ϕ_l is projected onto Φ_l to hold the new points in the feasible set. Specifically, the unit-modulus constraint means that ϕ_n^l has to be found inside the unit circle. $P_{\Phi_l}(\cdot)$ is the projection onto Φ_l . Hence, we have

$$\bar{u}_{l,n} = \begin{cases} \frac{u_{l,n}}{|u_{l,n}|} & u_{l,n} \neq 0 \\ e^{j\phi_n^l}, \phi_n^l \in [0, 2\pi] & u_{l,n} = 0 \end{cases}, n = 1, \dots, N, \quad (14)$$

where the vector $\bar{\mathbf{u}}_l$ of $P_{\Phi_l}(\mathbf{u}_l)$ is a given point.

The algorithm is described by the following iteration

$$\phi_l^{i+1} = P_{\Phi_l}(\phi_l^i + \mu_i \nabla_{\phi_l} f(\phi_l^i)). \quad (15)$$

The Armijo-Goldstein backtracking line search method provides the step size, which is $\mu_i = L_i \kappa^{m_i}$, where $\kappa \in (0, 1)$ and $L_i > 0$. Note that m_i is the smallest positive integer that satisfies

$$f(\phi_l^{i+1}) \geq Q_{L_i \kappa^{m_i}}(\phi_l^i; \phi_l^{i+1}), \quad (16)$$

where

$$Q_\mu(\phi_l; \mathbf{x}) = f(\phi_l) + \langle \nabla_{\phi_l} f(\phi_l), \mathbf{x} - \phi_l \rangle - \frac{1}{\mu} \|\mathbf{x} - \phi_l\|_2^2 \quad (17)$$

is the quadratic approximation of $f(\phi_l)$.

Proposition 2: The gradient of $f(\phi_l)$ regarding ϕ_l^* is obtained in closed-form as

$$\nabla_{\phi_l} f(\phi_l) = \frac{1}{\log_2(e)} \sum_{k=1}^K \frac{I_k \nabla_{\phi_l} D_k - D_k \nabla_{\phi_l} I_k}{(1 + \gamma_k) I_k}, \quad (18)$$

where

$$\nabla_{\phi_l} D_k = p_k \kappa_k \text{diag}(\mathbf{C}_l^* \mathbf{w}_k^{1*} \mathbf{w}_k^{1T} \mathbf{G}^T \mathbf{h}_{k,\text{LoS}}^* \mathbf{h}_{k,\text{LoS}}^T \mathbf{A}_l^*), \quad (19)$$

$$\begin{aligned} \nabla_{\phi_l} I_k &= \sum_{i=1}^K p_i \text{diag}(\mathbf{C}_l^* \mathbf{w}_i^{1*} \mathbf{w}_i^{1T} \mathbf{G}^T \mathbf{R} \mathbf{A}_l^*) \\ &+ \sum_{i \neq k}^K p_i \kappa_k \text{diag}(\mathbf{C}_l^* \mathbf{w}_i^{1*} \mathbf{w}_i^{1T} \mathbf{G}^T \mathbf{h}_{k,\text{LoS}}^* \mathbf{h}_{k,\text{LoS}}^T \mathbf{A}_l^*) \end{aligned} \quad (20)$$

with $\mathbf{A}_l = \Phi_L \mathbf{W}^L \dots \Phi_{l+1} \mathbf{W}^{l+1}$, and $\mathbf{C}_l = \mathbf{W}^l \Phi_{l-1} \mathbf{W}^{l-1} \dots \Phi_1$.

Proof: Please see Appendix A. \blacksquare

The SIM optimization design, based on the gradient ascent, appears a significant advantage because the gradient ascent is obtained in a closed form. It has low computational complexity because it consists of simple matrix operations. Specifically, the complexity of (13a) for large SIMs is $\mathcal{O}(N_t N^2 + L N^2 + K N^3)$, and the complexity of (18) is similar. In other words, the number of meta-atoms of each surface has a higher impact.

C. Power Optimization

Given a fixed Φ_l , we focus on the optimization with respect to \mathbf{p} . Specifically, we have

$$(\mathcal{P}2) \quad \max_{\mathbf{p}} f(\mathbf{p}) \quad (21a)$$

$$\sum_{i=1}^K p_i = P_T, p_k \geq 0, \forall k \in \mathcal{K}. \quad (21b)$$

The nonconvexity of problem ($\mathcal{P}2$) leads us to obtain a solution which is locally optimal. For this reason, we apply a weighted minimum mean square error (MMSE) reformulation of the sum SE. To this end, we denote $\mathbf{c} = [c_1, \dots, c_K]^T$. Then, the SINR γ_k can be written in terms of the vector \mathbf{p} as

$$\gamma_k = \frac{p_k q_k}{\mathbf{c}^T \mathbf{p} + u_k^2}, \quad (22)$$

where

$$\begin{aligned} q_k &= \kappa_k |\mathbf{h}_{k,\text{LoS}}^H \mathbf{G} \mathbf{w}_k^1|^2, c_k = \beta_k \frac{1}{1 + \kappa_k} \text{tr}(\mathbf{G} \mathbf{w}_k^1 \mathbf{w}_k^{1H} \mathbf{G}^H \mathbf{R}), \\ t_k^2 &= \frac{\sigma_k^2(1 + \kappa_k)}{\beta_k}, c_i = \beta_k \frac{1}{1 + \kappa_k} \text{tr}(\mathbf{G} \mathbf{w}_i^1 \mathbf{w}_i^{1H} \mathbf{G}^H \mathbf{R}) \\ &+ \beta_k \frac{\kappa_k}{1 + \kappa_k} \mathbf{h}_{k,\text{LoS}}^H \mathbf{G} \mathbf{w}_i^1 \mathbf{w}_i^{1H} \mathbf{G}^H \mathbf{h}_{k,\text{LoS}}, \forall i \neq k. \end{aligned} \quad (23)$$

Now, we consider the single-input and single-output (SISO) channel model that comes from the SINR in (22), which is given by

$$\tilde{y}_k = \sqrt{p_k q_k} s_k + \sum_{i=1}^K \sqrt{p_i c_i} s_i + n_k, \quad (24)$$

where $n_k \sim \mathcal{CN}(0, u_k^2)$ while $s_i \in \mathbb{C}$ is the data signal with unit variance, and \tilde{y}_k is the received signal.

Then, the receiver estimates s_k , i.e., $\hat{s}_k = v_k^* \tilde{y}_k$ with v_k being a receiver coefficient. The corresponding mean square error $e_k(\mathbf{p}, v_k) = \mathbb{E}[\|\hat{s}_k - s_k\|^2]$ becomes

$$e_k(\mathbf{p}, v_k) = v_{kg}^2 (p_k q_k + \mathbf{c}_k^T \mathbf{p} + u_k^2) - 2v_k \sqrt{q_k p_k} + 1. \quad (25)$$

For a given \mathbf{p} , v_k is obtained by the minimization of the MSE as

$$v_k = \frac{\sqrt{p_k q_k}}{p_k q_k + \sum_{i=1}^K p_i c_i + u_k^2}. \quad (26)$$

Inserting v_k into (25), e_k becomes $1/(1 + \gamma_k)$. Based on the weighted MMSE method, let the auxiliary weight $d_k \geq 0$ for the MSE e_k and consider the problem

$$\begin{aligned}
 (\mathcal{P}2.1) \quad & \min_{\substack{\mathbf{p} \geq 0, \\ \{v_k, d_k \geq 0; k=1, \dots, K\}}} K \sum_{k=1}^K d_k e_k(\mathbf{p}, \mathbf{v}_k) - \ln(d_k) \\
 & \text{s.t.} \quad \sum_{i=1}^K p_i \leq P_T.
 \end{aligned} \tag{27}$$

Problems (P2) and (P2.1) are equivalent, and thus, are subject to the same solution. The solution of (P2.1) can be provided in closed form as

$$p_i = \min \left(P_T, \frac{q_k d_k^2 v_k^2}{\left(q_k d_k v_k^2 + \sum_{i=1}^K d_i v_i^2 c_i \right)^2} \right). \tag{28}$$

The power allocation presents a similar complexity to the SIM optimization design since it consists of similar matrix operations to (P1), i.e., its complexity is $\mathcal{O}(N_t N^2 + L N^2 + K N^3)$.

Remark 1: Both algorithms, corresponding to Problems (P1) and (P2), have low computation complexity and converge quickly. Note that the achievement of a local optimum, obtained from this optimization, will make different initializations result in different solutions, which will be studied below.

V. NUMERICAL RESULTS

In this section, we present and evaluate the performance of the achievable sum SE of large SIM-assisted multiuser communications with statistical CSI by showing both analytical results and Monte Carlo simulations. For the setup, we assume that the SIM is parallel to the $x - y$ plane and centered along the z -axis at a height $H_{BS} = 10$ m. The spacing between adjacent meta-atoms is assumed to be $\lambda/2$, and the size of each meta-atom is $\lambda/2 \times \lambda/2$. The thickness of the SIM is $T_{SIM} = 5\lambda$, while the spacing is $d_{SIM} = T_{SIM}/L$. Moreover, the locations of the users are randomly distributed at a distance between 60m and 80m.

The distance between the \tilde{n} -th meta-atom of the $(l-1)$ -st metasurface and the n -th meta-atom of the l -st metasurface is given by $d_{n,\tilde{n}}^l = \sqrt{d_{SIM}^2 + d_{n,\tilde{n}}^2}$, where

$$d_{n,\tilde{n}} = \frac{\lambda}{2} \sqrt{[|n - \tilde{n}|/N_x]^2 + [\text{mod}(|n - \tilde{n}|, N_x)]^2}. \tag{29}$$

The transmission distance between the m -th antenna and the \tilde{n} -th meta-atom on the first metasurface layer is provided by (30). Note that we have $\cos x_{n,\tilde{n}}^l = d_{SIM}/d_{n,\tilde{n}}^l, \forall l \in \mathcal{L}$.

The path loss is given by

$$\tilde{\beta}_k = C_0 (d_k/\hat{d})^{-\alpha}, \tag{31}$$

where $C_0 = (\lambda_2/4\pi\hat{d})$ is the free space path loss at the reference distance of $\hat{d} = 1$ m, and $\alpha = 2.5$ is the path-loss exponent. The correlation matrix \mathbf{R}_{SIM} is obtained according to (4). The carrier frequency and the system bandwidth are 2 GHz and 20 MHz, respectively. Moreover, we assume $N_t = 8$, $K = 8$, $N = 200$, and $L = 4$.

In Fig. 2, we depict the achievable sum SE versus the number of elements N of each surface while varying the number of surfaces L . First, it is shown that the downlink sum SE increases with N for different L . Moreover, an increase

in the number of surfaces results in an increase in the sum SE. In addition, for the sake of comparison, we present the performance in the case of instantaneous CSI for $L = 4$ [8], which performs better than the case of statistical CSI since the latter is obtained based on a lower bound that is optimized at every several coherence intervals instead of at each coherence interval. However, the statistical CSI modeling allows to save significant overhead. Moreover, we show the effect of the size of each surface element. We observe that as the size of each surface element decreases, the correlation decreases, and the sum SE increases. Notably, Monte Carlo (MC) simulations corroborate the analytical results.

Fig. 3 shows the sum SE versus the number of layers L of the SIM for the number of UEs K . When $N_t = K = 8$, we observe that the sum SE improves until $L = 6$ because the SIM is able to mitigate the inter-user interference in the EM wave domain. In particular, a significant improvement is observed compared to the single-layer SIM. Again, we illustrate the comparison between the cases corresponding to instantaneous and statistical CSI, where the latter exhibits worse performance for the benefit of lower overhead.

In Fig. 4, we depict the convergence of the proposed algorithm. The algorithm terminates when the difference of the objective between the two last iterations is less than 10^{-5} or the number of iterations is larger than 130. It is shown that the algorithm converges to its maximum as the number of iterations increases. Since Problem (P) is non-convex, the algorithm does not converge to a globally optimal solution. This means that the algorithm may converge to different points starting from different initial points. For this reason, we select the best solutions after executing the algorithm from different initial points. Herein, we depict the sum SE versus the iteration count for 5 different randomly generated initial points, and we observe that all points result in the same SE. Generally, the selection of 5 randomly generated initial points allows a good trade-off between performance and complexity.

VI. CONCLUSION

This paper provided the achievable downlink SE of large SIM-aided multiuser communications over Ricean fading channels. In particular, we deduced a new, tractable expression for the downlink SE for large-metasurfaces as a function of large-scale statistics while the downlink precoding takes place in the wave domain, in order to lower the computational burden and the processing latency. The results were used to pursue an optimization based on statistical CSI that achieves lower overhead with respect to instantaneous CSI. Specifically, we proposed an AO algorithm that solves the optimization regarding the phase shifts of each surface of the SIM and the allocated power, which contributes to a reduction in processing latency due to lower overhead.

APPENDIX A PROOF OF PROPOSITION 2

The proof starts with the derivation of $\nabla_{\phi_l} D_k$. To this end, we focus on the differential of $|\mathbf{h}_{k,\text{LoS}}^H \mathbf{G} \mathbf{w}_k|^2$. We have

$$\begin{aligned}
 d(|\mathbf{h}_{k,\text{LoS}}^H \mathbf{G} \mathbf{w}_k|^2) &= \mathbf{h}_{k,\text{LoS}}^H d(\mathbf{G}) \mathbf{w}_k \mathbf{w}_k^H \mathbf{G}^H \mathbf{h}_{k,\text{LoS}} \\
 &+ \mathbf{h}_{k,\text{LoS}}^H \mathbf{G} \mathbf{w}_k \mathbf{w}_k^H d(\mathbf{G}^H) \mathbf{h}_{k,\text{LoS}}
 \end{aligned} \tag{32}$$

$$\begin{aligned}
 &= \text{tr} \left(\mathbf{h}_{k,\text{LoS}}^H \mathbf{A}_l d(\Phi_l) \mathbf{C}_l \mathbf{w}_k \mathbf{w}_k^H \mathbf{G}^H \mathbf{h}_{k,\text{LoS}} \right) \\
 &+ \text{tr} \left(\mathbf{A}_l^H \mathbf{h}_{k,\text{LoS}} \mathbf{h}_{k,\text{LoS}}^H \mathbf{G} \mathbf{w}_k \mathbf{w}_k^H \mathbf{C}_l^H d(\Phi_l^H) \right).
 \end{aligned} \tag{33}$$

$$d_{\tilde{n},m}^1 = \sqrt{d_{\text{SIM}}^2 + \left[\left(\text{mod}(\tilde{n}-1, N_x) - \frac{N_x-1}{2} \right) \frac{\lambda}{2} - \left(m - \frac{N_t+1}{2} \right) \frac{\lambda}{2} \right]^2 + \left(\lceil \tilde{n}/N_x \rceil - \frac{N_y+1}{2} \right)^2 \frac{\lambda_2}{4}}. \quad (30)$$

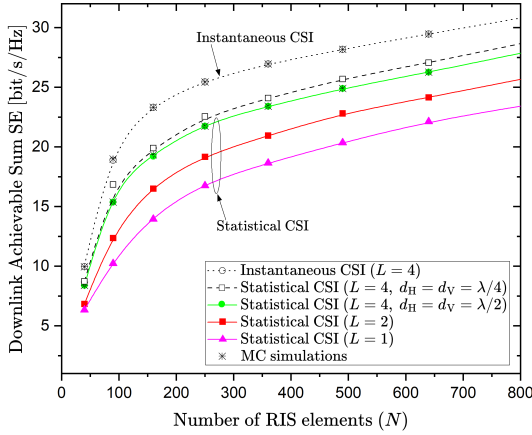


Fig. 2: Achievable sum SE of the large SIM-aided MIMO architecture with respect to the number of meta-atoms N .

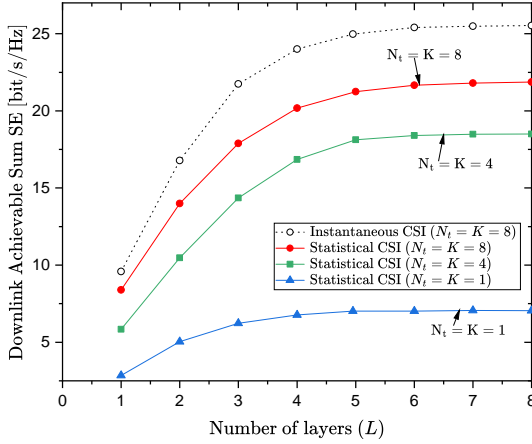


Fig. 3: Achievable sum SE of the large SIM-aided MIMO architecture with respect to the number of meta-surfaces L .

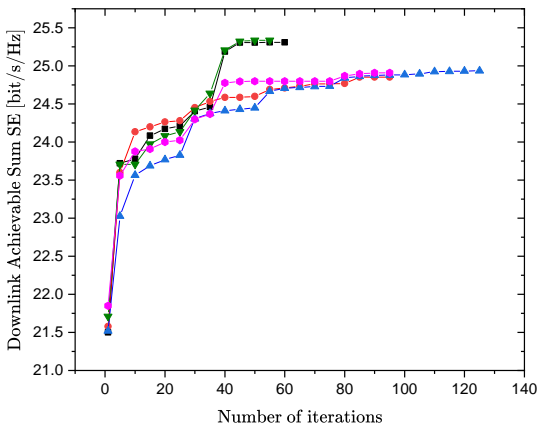


Fig. 4: Achievable sum SE of the large SIM-aided MIMO architecture with respect to the number of iterations for 5 different randomly generated initial points.

In (33), we have substituted $d(\mathbf{G}) = \mathbf{A}_l d(\Phi_l) \mathbf{C}_l$, where $\mathbf{A}_l = \Phi_L \mathbf{W}^L \dots \Phi_{l+1} \mathbf{W}^{l+1}$, and $\mathbf{C}_l = \mathbf{W}^l \Phi_{l-1} \mathbf{W}^{l-1} \dots \Phi_1$. Having obtained the differential, we have

$$\nabla_{\phi_l} D_k = \frac{\partial}{\partial \phi_l^*} D_k \quad (34)$$

$$= p_k \kappa_k \text{diag}(\mathbf{C}_l^* \mathbf{w}_k^{1*} \mathbf{w}_k^{1\top} \mathbf{G}^\top \mathbf{h}_{k,\text{LoS}}^* \mathbf{h}_{k,\text{LoS}}^\top \mathbf{A}_l^*). \quad (35)$$

The first term in the denominator is written as

$$d(\text{tr}(\mathbf{G} \mathbf{w}_i^1 \mathbf{w}_i^{1\text{H}} \mathbf{G}^\text{H} \mathbf{R})) = \text{tr}(\mathbf{A}_l d(\Phi_l) \mathbf{C}_l \mathbf{w}_i^1 \mathbf{w}_i^{1\text{H}} \mathbf{G}^\text{H} \mathbf{R}) + \text{tr}(\mathbf{A}_l^\text{H} \mathbf{R} \mathbf{G} \mathbf{w}_i^1 \mathbf{w}_i^{1\text{H}} \mathbf{C}_l^\text{H} d(\Phi_l^*)). \quad (36)$$

Thus, we have

$$\nabla_{\phi_l} \text{tr}(\mathbf{G} \mathbf{w}_i^1 \mathbf{w}_i^{1\text{H}} \mathbf{G}^\text{H} \mathbf{R}) = \text{diag}(\mathbf{C}_l^* \mathbf{w}_i^{1*} \mathbf{w}_i^{1\top} \mathbf{G}^\text{H} \mathbf{R} \mathbf{A}_l^*). \quad (37)$$

The second term in the denominator is similar to the numerator. Hence, the derivation is similar.

REFERENCES

- [1] M. Di Renzo *et al.*, “Smart radio environments empowered by reconfigurable intelligent surfaces: How it works, state of research, and the road ahead,” *IEEE J. Sel. Areas Commun.*, vol. 38, no. 11, pp. 2450–2525, 2020.
- [2] Y. Liu *et al.*, “Reconfigurable intelligent surfaces: Principles and opportunities,” *IEEE Commun. Surveys & Tuts.*, vol. 23, no. 3, pp. 1546–1577, 2021.
- [3] C. Huang *et al.*, “Reconfigurable intelligent surfaces for energy efficiency in wireless communication,” *IEEE Trans. Wireless Commun.*, vol. 18, no. 8, pp. 4157–4170, 2019.
- [4] A. Papazafeiropoulos *et al.*, “Intelligent reflecting surface-assisted MU-MISO systems with imperfect hardware: Channel estimation and beamforming design,” *IEEE Trans. Wireless Commun.*, vol. 21, no. 3, pp. 2077–2092, 2021.
- [5] —, “Achievable rate of a STAR-RIS assisted massive MIMO system under spatially-correlated channels,” *IEEE Trans. Wireless Commun.*, pp. 1–1, 2023.
- [6] H. Guo *et al.*, “Weighted sum-rate maximization for reconfigurable intelligent surface aided wireless networks,” *IEEE Trans. Wireless Commun.*, vol. 19, no. 5, pp. 3064–3076, 2020.
- [7] J. An *et al.*, “Stacked intelligent metasurfaces for efficient holographic MIMO communications in 6G,” *IEEE J. Sel. Areas Commun.*, 2023.
- [8] —, “Stacked intelligent metasurfaces for multiuser downlink beamforming in the wave domain,” *arXiv preprint arXiv:2309.02687*, 2023.
- [9] A. Papazafeiropoulos *et al.*, “Achievable rate optimization for stacked intelligent metasurface-assisted holographic MIMO communications,” *arXiv preprint arXiv:2402.16415*.
- [10] A. Papazafeiropoulos, P. Kourtessis, and S. Chatzinotas, “Performance of double-stacked intelligent metasurface-assisted multiuser massive MIMO communications in the wave domain,” *arXiv preprint arXiv:2402.16405*, 2024.
- [11] S. Lin *et al.*, “Stacked intelligent metasurface enabled LEO satellite communications relying on statistical CSI,” *IEEE Wireless Commun. Lett.*, 2024.
- [12] E. Björnson *et al.*, “Massive MIMO networks: Spectral, energy, and hardware efficiency,” *Foundations and Trends® in Signal Processing*, vol. 11, no. 3–4, pp. 154–655, 2017.
- [13] C. Liu *et al.*, “A programmable diffractive deep neural network based on a digital-coding metasurface array,” *Nature Electronics*, vol. 5, no. 2, pp. 113–122, 2022.
- [14] E. Björnson and L. Sanguinetti, “Rayleigh fading modeling and channel hardening for reconfigurable intelligent surfaces,” *IEEE Wireless Commun. Lett.*, vol. 10, no. 4, pp. 830–834, 2021.